arXiv:cond-mat/0212493v1 [cond-mat.str-el] 19 Dec 2002

Wilson-Kadanoff Renormalization Group in Higher Orders: One-Dimensional g-ology Model as an Example

Gennady Y. Chitov*

Centre de recherche sur les propriétés électoniques de matériaux avancés, Université de Sherbrooke, Sherbrooke, Québec, Canada J1K 2R1 and

Physics Department, McGill University, Montréal, Québec, Canada H3A 2T8

Claude Bourbonnais

Centre de recherche sur les propriétés électoniques de matériaux avancés, Université de Sherbrooke, Sherbrooke, Québec, Canada J1K 2R1

(Dated: February 1, 2008)

Abstract

We apply the standard Wilson-Kadanoff (WK) momentum-space Renormalization Group (RG) scheme for the g-ology model of one-dimensional fermions. By explicitly carrying out calculations at the two-loop level, we show how the RG flow equations can be derived from the summation of the cascades of contractions generated by the effective action's mode elimination at each infinitesimal step of the WK procedure. The rules for selecting these series of cascades appear naturally as a consequence of the WK scheme "on-shell" kinematic constraints and conservation laws. The relation between the present RG approach and the field-theoretic schemes used in earlier related studies is analysed. Generalizations for other models and/or higher dimensions are formulated.

PACS numbers: 05.30.Fk, 71.10Pm, 11.10.Hi, 05.10.Cc

*Present address: Department 7.1-Theoretical Physics, University of the Saarland, Saarbrücken 66041, Germany

I. INTRODUCTION

The Renormalization Group (RG) approach, in its most enlightening formulation due to Wilson [1, 2], is the theory designed to handle fields (quantum or classical) fluctuating over range of momentum (energy) scales.[1] In the momentum-space formulation, this range of scales where fluctuations matter is bounded by some initial ultraviolet (UV) cutoff Λ_0 (not necessarily finite) provided by the problem under consideration, and Λ_0 is the scale where the RG procedure of the successive mode integration starts. For the most problems where RG was successfully applied (e.g., phase transition, field theories) the low-energy sector of interest resides near one point of the momentum space which can always be mapped to the origin of that space.

In practical loopwise calculations, the original WK infinitesimal scheme seems however to appear too involved beyond one-loop level, and, e.g., for the Wilson's original problem of phase transition in higher orders various field-theoretic RG approaches were applied [4]. In field theory the cutoff Λ_0 is essentially considered as a "troublesome" parameter to get rid of, either by eventually taking the limit $\Lambda_0 \to \infty$, or, e.g, by using another regularization scheme, like the dimensional one where the cutoff is set to infinity from the start.

Contrary to the WK scheme, which specifically stipulates that at each RG step the momenta to be integrated out lie within infinitesimally narrow shell in the momentum space, in the field-theoretic RG only overall momentum conservation is taken care of, while separate momenta may lie outside of the (hyper)sphere of radius Λ (centered at the origin). This situation is well known, and contributions from the states lying outside of the action's phase space at the distance of several radii Λ– or, in other terms, violating phase space constraints by $\mathcal{O}(\Lambda)$– do not affect the leading terms of the RG flow.

However, in condensed matter problems the Wilsonian *effective action's scale* Λ_0 must be taken seriously. *A priori* it cannot be set to infinity or even to the largest scale provided by the underlying microscopics, i.e., inverse lattice, interatomic, etc, spacing. Even for a problem with the low-energy sector localized near the origin of the momentum space, aforementioned violations of the phase space constraints result in double counting of the degrees of freedom lying outside of the Wilsonian phase space (i.e., the degrees of freedom which are already "integrated out" in some way before we reached the Wilsonian scale from the microscopic scale). This can affect the next-to-leading terms, as well as finite renormalizations of the action's parameters.

For the important problem of fermions having a Fermi surface – that is a low-energy sector residing near a manifold in the momentum space – accounting for the modes within the phase space *only* during the RG procedure becomes a rather non-trivial task, as was explained by Shankar [5]. Moreover, the error of violating the phase space constraints can be of order $\mathcal{O}(K_F)$, where K_F is some characteristic size of the Fermi surface, even if the low-energy modes we are integrating out reside within a narrow shell $\Lambda \ll K_F$.

Note that the answers for many of the most interesting problems of the condensed-matter fermions lie in calculating the abovementioned "next-to-leading terms", where the differences between various RG approaches matter. For instance, the problem of the Fermi-Liquid vs non-Fermi-Liquid regimes of the normal state of the cuprates, from an RG point of view is

[1] Since the Wilson RG theory was strongly motivated by Kadanoff's more intuitive original approach of successive averaging of the spin Hamiltonian in real space [3], it is often called the Wilson-Kadanoff (WK) RG, the term we apply in this study.

the difference in the behavior of the irrelevant (self-energy) terms in both regimes. So the choice of the optimal RG scheme and the control over the subleading terms are the issues far from being academical.

The main claim we want to make from the considerations of this paper is that for a condensed-matter problem cast in terms of the Wilsonian effective action with a physically meaningful UV cutoff Λ_0, the WK RG provides the only scheme definitely reliable in all orders of the loopwise expansions, where all modes from the phase space are integrated once and only once. (Strictly speaking, there are no new results in the RG equations we derive below, since for the g-ology model they have been known for a long time, either from field-theoretical RG scheme [6, 7] or more recent WK RG formulations [8]). We address the issues of how to practically employ the WK RG in higher orders, to which technically simpler scheme the WK RG can be reduced and to what extend, by studying the g-ology model of 1D fermions.

The model we consider is the simplest case of the condensed-matter fermions where the Fermi surface manifold is just a set of two points. By going deeper into a recent suggestion to this problem [9], we apply a WK RG transformation assuring that at each step of the procedure all momenta lie within the infinitesimal shell of integration and satisfy the conservation laws, so there are no contributions from the extra states nor double counting. We show how the higher order renormalizations of the effective action's parameters appear from the summation of the cascades of contractions generated at each step of the WK procedure. We don't go beyond the two-loop level, which is apparently the optimal one for feasible calculations. At this level, we show that the summations over the cascades in the WK scheme is equivalent (in the fixed-point limit of the decreasing cutoff $\Lambda \to 0$) to applying the cutoff regularization for the field-theoretic RG *with the extra states excluded from the phase space*. This result, to the best of our knowledge, was not explicitly shown before. Considerable simplifications for our analysis came from introducing the chiral matrix formalism. This is a naïve (for the simple 1D case) first attempt to build into the technique the disentanglement of geometry (characterized by the "large" rigid scale K_F) and the low-energy sector *per se* (characterized by the decreasing scale Λ), and to map the latter to the same origin. This mapping makes the exclusion of the extra states particularly simple.

The rest of this paper is organized as follows. Sections II A-II D are introductory. Section II A defines the effective action. In Section II B the chiral matrix formalism is introduced. In Section II D we explain the terms and notations of the Wilson-Kadanoff RG as it is applied in this paper. In Sections III A-III B we explain the procedure and give the results for the two-loop self-energy calculations, and in Sections III C we establish the relationship between the field-theoretic RG and the present approach. Section IV contains the two-loop results for the couplings flow equations. The conclusions and generalizations for other models and/or higher dimensions are presented in the final Section V.

II. MODEL AND FORMALISM

A. $SU(N)$-invariant d-dimensional ψ^4-action

We treat d-dimensional interacting fermions at finite temperature in the standard path integral Grassmannian formalism [10]. The $SU(N)$-invariant fermionic ψ^4-action along with the related quantities and notations of this subsection have been introduced earlier [11], and

we recall these here in order to make the paper self-contained. The partition function is

$$\mathcal{Z} = \int \mathcal{D}\bar{\psi}\mathcal{D}\psi \; e^{S_0+S_{\rm int}} \tag{1}$$

The free part of the action is

$$S_0 = \int_{(\mathbf{1})} \bar{\psi}_\alpha(\mathbf{1}) \left[i\omega_1 + \mu - \epsilon(\mathbf{K}_1) \right] \psi_\alpha(\mathbf{1}) \tag{2}$$

and $(d+1)$-dimensional vectors and integrals mean

$$\int_{(\mathbf{i})} \equiv \frac{1}{\beta} \int \frac{d\mathbf{K}_i}{(2\pi)^d} \sum_{\omega_i} \tag{3a}$$

$$(\mathbf{i}) \equiv (\mathbf{K}_i, \omega_i) \tag{3b}$$

where β is the inverse temperature, μ the chemical potential, ω_i the fermion Matsubara frequencies and $\psi_\alpha(\mathbf{i})$ a N-component Grassmann field with a spin (flavor, if $N \neq 2$) index α. Summation over repeated indices is implicit throughout this paper. We set $k_B = 1$ and $\hbar = 1$. The $SU(N)$-invariant quartic interaction is

$$S_{\rm int} = -\frac{1}{4} \int_{(\mathbf{1},\mathbf{2},\mathbf{3},\mathbf{4})} \bar{\psi}_\alpha(\mathbf{1}) \bar{\psi}_\beta(\mathbf{2}) \psi_\gamma(\mathbf{3}) \psi_\varepsilon(\mathbf{4}) U^{\alpha\beta}_{\gamma\varepsilon}(\mathbf{1},\mathbf{2};\mathbf{3},\mathbf{4}) \delta^{(d+1)}(\mathbf{1}+\mathbf{2}-\mathbf{3}-\mathbf{4}) \tag{4}$$

Here the conservation of energy and momentum is enforced by the symbolic delta function

$$\delta^{(d+1)}(\mathbf{1}+\mathbf{2}-\mathbf{3}-\mathbf{4}) \equiv \beta(2\pi)^d \delta(\mathbf{K}_1+\mathbf{K}_2-\mathbf{K}_3-\mathbf{K}_4) \delta_{\omega_1+\omega_2-\omega_3-\omega_4,0} \tag{5}$$

Note that for the lattice fermions the delta-function above conserves momenta up to an inverse lattice vector. The physical case of the spin-$\frac{1}{2}$ electrons is recovered by setting $N = 2$. We decompose the interaction by factorizing its symmetric and antisymmetric frequency-momentum- and spin- dependent parts as

$$U^{\alpha\beta}_{\gamma\varepsilon} = U^A I^{\alpha\beta}_{\gamma\varepsilon} + U^S T^{\alpha\beta}_{\gamma\varepsilon} \tag{6}$$

where the functions $U^{S/A}$ are symmetric/antisymmetric under exchange of the left or right pairs of their variables. Two operators $\hat{I}$ and $\hat{T}$, which are respectively symmetric and antisymmetric in the spin space, are defined as follows:

$$I^{\alpha\beta}_{\gamma\varepsilon} \equiv \delta_{\alpha\varepsilon}\delta_{\beta\gamma} + \delta_{\alpha\gamma}\delta_{\beta\varepsilon} \tag{7a}$$

$$T^{\alpha\beta}_{\gamma\varepsilon} \equiv \delta_{\alpha\varepsilon}\delta_{\beta\gamma} - \delta_{\alpha\gamma}\delta_{\beta\varepsilon} \tag{7b}$$

The one-particle-irreducible (1PI) four-point vertex $\hat{\Gamma}$, defined in the standard way, comprises two components (Γ^A, Γ^S) and can be written in the same manner as (6). Along with such representation showing explicitly its antisymmetry, there is another one which separates the vertex into charge and spin components via

$$\hat{\Gamma} \mapsto \Gamma^{\alpha\beta}_{\gamma\varepsilon} = \Gamma^A I^{\alpha\beta}_{\gamma\varepsilon} + \Gamma^S T^{\alpha\beta}_{\gamma\varepsilon} = -\frac{1}{N}\Gamma_{\rm c}\delta_{\alpha\gamma}\delta_{\beta\varepsilon} - \frac{1}{2}\Gamma_{\rm s}\lambda^a_{\alpha\gamma}\lambda^a_{\beta\varepsilon} \tag{8}$$

The latter representation is often more convenient since charge and spin components decouple in many practical calculations. $\hat{\lambda}^a$ $(a = 1, ..., N^2 - 1)$ in Eq.(8) are Hermitian traceless generators of the $SU(N)$ group, coinciding with the Pauli matrices for $N = 2$, and normalized such that

$$\mathrm{tr}(\hat{\lambda}^a \hat{\lambda}^b) = 2\delta^{ab} \tag{9}$$

They also satisfy the following Fierz identity:

$$\lambda^a_{\alpha\beta}\lambda^a_{\gamma\varepsilon} = 2\Big(\delta_{\alpha\varepsilon}\delta_{\beta\gamma} - \frac{1}{N}\delta_{\alpha\beta}\delta_{\gamma\varepsilon}\Big) \tag{10}$$

The components of the vertex in different representations are related as

$$\Gamma_{\rm c} \;=\; (N-1)\Gamma^S - (N+1)\Gamma^A \tag{11a}$$
$$\Gamma_{\rm s} \;=\; -\Gamma^S - \Gamma^A \tag{11b}$$

B. Chiral matrix formalism for the 1D effective action

The construction of the low-energy effective fermionic action as a simplified form of the generic ψ^4-action (2,4) reduces in 1D essentially to the three key steps: extraction of a finite set of (marginal) couplings; decomposition of the physical electron ψ-field into two chiral fields "near" left and right Fermi points; linearization of the one-particle spectrum $\epsilon(K)$ around these points. There exists an extensive literature on the derivation of the 1D effective action models (Tomonaga-Luttinger, g-ology), and on many subtleties it involves (see, e.g., Ref.[12] and more references therein). So below we simply present notations, approximations and highlight the main points. The chiral matrix representation we derive here is in fact only a way to re-write the well-known g-ology model. (For details see the next subsection.) However this matrix formalism and related to it diagrammatics help to facilitate bookkeeping of diagrams and handling their contributions to different couplings, and, eventually, to generalize the g-ology results for other cases.

We decompose 1D momenta as

$$K_i \equiv p_i K_F + k_i \tag{12}$$

where $p_i = sign(K_i) = \pm 1$ corresponds to the right (R) /left (L) Fermi points. In the quartic interaction function $\hat{U}(\mathbf{1}, \mathbf{2}; \mathbf{3}, \mathbf{4})$ (6) we retain only its dependence on the momenta at the Fermi points, neglecting that on k_i-s and frequencies [13]. The $SU(N)$ and exchange symmetry constraints leave us with four independent marginal couplings:

$$g^A \;\equiv\; U^A(LR;LR) = -U^A(RL;LR) = -U^A(LR;RL) \tag{13a}$$
$$g^S \;\equiv\; U^S(LR;LR) = \;\; U^S(RL;LR) = \;\; U^S(LR;RL) \tag{13b}$$
$$g_4 \;\equiv\; U^S(LL;LL) = U^S(RR;RR) \tag{13c}$$
$$g_3 \;\equiv\; U^S(LL;RR) = U^S(RR;LL) \tag{13d}$$

Note that the Umklapp coupling g_3 is operative only in the half-filled case when $4K_F = 2\pi$ (we set the lattice constant $a = 1$). For the formalism we develop below this case is considered as the most general one, while the non-commensurate filling can be recovered by setting $g_3 = 0$.

We introduce left (right) chiral Grassmannian fields as:

$$\psi_\alpha(\mp K_F + k_i, \omega_i) = \psi_\alpha^{L/R}(k_i, \omega_i) \tag{14}$$

Small vectors

$$k_i \in [-\Lambda_0, \Lambda_0] \tag{15}$$

are restricted by the bare momentum cutoff Λ_0 of the effective action. Then the effective quartic interaction [cf. Eq.(4)] can be represented as

$$S_{\rm eff}^{(4)} = -\frac{1}{4}\int_{(1,2,3,4)} \mathcal{L}_{\rm eff}^{(4)}\ \delta^{(1+1)}(1+2-3-4) \tag{16}$$

where the transition from bold to thin variables corresponds to $K_i \mapsto k_i$ [cf. notations (3,5,12)], and

$$\begin{aligned}
\mathcal{L}_{\rm eff}^{(4)} \ &= \ \bar\psi_\alpha^L(1)\bar\psi_\beta^L(2)\psi_\gamma^L(3)\psi_\varepsilon^L(4)[\quad 0\cdot I_{\gamma\varepsilon}^{\alpha\beta} + g_4\cdot T_{\gamma\varepsilon}^{\alpha\beta}] + (L\leftrightarrow R)\\
&+\ \bar\psi_\alpha^L(1)\bar\psi_\beta^L(2)\psi_\gamma^R(3)\psi_\varepsilon^R(4)[\quad 0\cdot I_{\gamma\varepsilon}^{\alpha\beta} + g_3\cdot T_{\gamma\varepsilon}^{\alpha\beta}] + (L\leftrightarrow R)\\
&+\ \bar\psi_\alpha^L(1)\bar\psi_\beta^R(2)\psi_\gamma^L(3)\psi_\varepsilon^R(4)[\ g^A\cdot I_{\gamma\varepsilon}^{\alpha\beta} + g^S\cdot T_{\gamma\varepsilon}^{\alpha\beta}] + (L\leftrightarrow R)\\
&+\ \bar\psi_\alpha^L(1)\bar\psi_\beta^R(2)\psi_\gamma^R(3)\psi_\varepsilon^L(4)[-g^A\cdot I_{\gamma\varepsilon}^{\alpha\beta} + g^S\cdot T_{\gamma\varepsilon}^{\alpha\beta}] + (L\leftrightarrow R)
\end{aligned} \tag{17}$$

Note that the delta-function in (16), contrary to its "bold" counterpart (5), conserves the small momenta k_i exactly, since the lattice effects at half-filling (g_3-terms) are explicitly taken into account in (17).

Let us now introduce four 2×2 matrices $\hat t^i$ such that $\hat t^0$ is the unit matrix, and $\hat t^i$ for $i=1,2,3$ correspond to the Pauli matrices. Such distinct notation helps to avoid confusion, since $\hat t^i$ operates in the chiral, and not in the spin space. We attribute an extra chiral index to the Grassmannian field as $L\mapsto 1$, $R\mapsto 2$. Then four terms in the last two lines of Eq.(17) can be written as:

$$\mathcal{L}_{\rm fb} = [-g^A\cdot I_{\gamma\varepsilon}^{\alpha\beta}\cdot t^2_{\alpha'\beta'}t^2_{\gamma'\varepsilon'} + g^S\cdot T_{\gamma\varepsilon}^{\alpha\beta}\cdot t^1_{\alpha'\beta'}t^1_{\gamma'\varepsilon'}]\ \bar\psi_\alpha^{\alpha'}(1)\bar\psi_\beta^{\beta'}(2)\psi_\gamma^{\gamma'}(3)\psi_\varepsilon^{\varepsilon'}(4) \tag{18}$$

while the first two lines in that equation give

$$\mathcal{L}_{\rm uc} = T_{\gamma\varepsilon}^{\alpha\beta}\cdot[g_p\cdot t^0_{\alpha'\beta'}t^0_{\gamma'\varepsilon'} + g_m\cdot t^3_{\alpha'\beta'}t^3_{\gamma'\varepsilon'}]\ \bar\psi_\alpha^{\alpha'}(1)\bar\psi_\beta^{\beta'}(2)\psi_\gamma^{\gamma'}(3)\psi_\varepsilon^{\varepsilon'}(4) \tag{19}$$

where

$$g_{p/m} \equiv \frac{1}{2}(g_4 \pm g_3) \tag{20}$$

Thus

$$\mathcal{L}_{\rm eff}^{(4)} = \mathcal{L}_{\rm fb} + \mathcal{L}_{\rm uc} \tag{21}$$

The one-particle Green's function is spin-independent in the model we consider, but it depends on the chiral index:

$$-\langle\psi_\gamma^\alpha(1)\bar\psi_\varepsilon^\beta(2)\rangle = G_\alpha(1)\delta_{\alpha\beta}\delta_{\gamma\varepsilon}\delta^{(1+1)}(1-2) \tag{22}$$

The linearized bare Green's function is given by

$$G_{0,\alpha}^{-1}(k_n,\omega_n) = i\omega_n + \mu - \epsilon(p_\alpha K_F + k_n) \approx i\omega_n - p_\alpha v_F k_n \tag{23}$$

where

$$p_\alpha = 2(\alpha - 1) - 1 \tag{24}$$

Now we can define the 1PI four-point vertex $\hat{\Gamma}$ in this formalism. We will be interested in a particular limiting form of this vertex when its dependence on the external momenta lying at the Fermi points (parametrized by the chiral indices) is retained only, while (k_n, ω_n) are discarded. In the lowest order $\hat{\Gamma}^{(0)}$ can be read off from $\mathcal{L}^{(4)}_{\text{eff}}$ (18,19,21). As follows from the group-theory arguments, this structure of the vertex is preserved by interaction $\mathcal{L}^{(4)}_{\text{eff}}$: the latter results in only the renormalization of couplings, but no new couplings are generated. Thus, the following operator expansion with four couplings holds non-perturbatively:

$$\hat{\Gamma} = -g^A\ \hat{I} \otimes \hat{t}^2 \otimes \hat{t}^2 + \hat{T} \otimes [g^S\ \hat{t}^1 \otimes \hat{t}^1 + g_p\ \hat{t}^0 \otimes \hat{t}^0 + g_m\ \hat{t}^3 \otimes \hat{t}^3] \tag{25}$$

In order to keep the notations compact, we do not change them in (25), however couplings are renormalized by interaction comparatively to their bare values (13). To the same end we will not indicate explicitly the chiral and spin indices from now on (unless there is a possibility of confusion), incorporating them into the "thin variables". So we imply

$$\mathcal{L}_{\text{fb}} + \mathcal{L}_{\text{uc}} \mapsto\ \text{[cf. Eqs.(18,19)]}\ \mapsto \Gamma^{(0)}(12;34)\bar{\psi}(1)\bar{\psi}(2)\psi(3)\psi(4) \tag{26}$$

Comparison of Eqs.(18,19,26) with the operator form (25) clarifies how we attribute the chiral and spin indices for the matrix elements of $\hat{\Gamma}$. Note the explicit antisymmetry of the vertex $\Gamma(12;34)$ under exchange of the left or right pairs of variables in the representation (25).

We can recover couplings from the vertex by appropriate convolutions, i.e.,

$$g^A\ =\ -\frac{1}{48}\Big(t^2_{21} \cdot \Gamma(12;34) \cdot I^{43}_{21} \cdot t^2_{43}\Big) \tag{27a}$$

$$g_p\ =\ \ \frac{1}{16}\Big(t^0_{21} \cdot \Gamma(12;34) \cdot T^{43}_{21} \cdot t^0_{43}\Big) \tag{27b}$$

and other two couplings are obtained from Eq.(27b) by obvious substitutions, namely, $g^S:\ \hat{t}^0 \mapsto \hat{t}^1$; $g_m:\ \hat{t}^0 \mapsto \hat{t}^3$.

C. Contact with the g-ology model

Here we want to make a contact between the chiral matrix formalism and more commonly used g-ology language (see, e.g., Ref.[7]). No surprise that this subsection's formal manipulations with the fully (anti)symmetrized "chiral" action amount essentially to reducing it to the non-symmetrized form. The latter is usually used as a departure point of various g-ology models.

Let us show first how the charge- and spin-operator interaction action, involving forward and backscattering couplings called g_2, g_1 respectively in the g-ology nomenclature, can be recovered from the part $\mathcal{L}_{\text{fb}}$ (18) of the effective quartic interaction (21). $\mathcal{L}_{\text{fb}}$ can be split in two terms by the following projection in the chiral space:

$$\begin{aligned}\mathcal{L}_{\text{fb}}\ &=\ \Big([1 - t^0_{\alpha\gamma}t^0_{\beta\varepsilon}] + t^0_{\alpha\gamma}t^0_{\beta\varepsilon}\Big)(-g^A\hat{I}\ t^2_{\alpha\beta}t^2_{\gamma\varepsilon} + g^S\hat{T}\ t^1_{\alpha\beta}t^1_{\gamma\varepsilon})[\psi^4]_N \\ &\equiv\ \mathcal{L}_{\text{cs1}} + \mathcal{L}_{\text{cs2}}\end{aligned} \tag{28}$$

Above we indicate explicitly the chiral indices only, and $[\psi^4]_N$ stands for the product of four ψ-fields "normally-ordered" as on the r.h.s. of Eq.(18). Using the Fierz identity (10) for the $SU(2)$ chiral operators t^i, one can prove that

$$\begin{aligned}\mathcal{L}_{\rm cs1} &\equiv (1-t^0_{\alpha\gamma}t^0_{\beta\varepsilon})(-g^A\hat{I}\ t^2_{\alpha\beta}t^2_{\gamma\varepsilon}+g^S\hat{T}\ t^1_{\alpha\beta}t^1_{\gamma\varepsilon})[\psi^4]_N \\ &= \frac{1}{2}(t^1_{\alpha\beta}t^1_{\gamma\varepsilon}+t^2_{\alpha\beta}t^2_{\gamma\varepsilon})(-g^A\hat{I}+g^S\hat{T})[\psi^4]_N \end{aligned} \tag{29}$$

It can be also shown that the above expression reduces to

$$\mathcal{L}_{\rm cs1} = t^1_{\alpha\beta}(-g^A\hat{I}+g^S\hat{T})\bar{\psi}^\alpha(1)\bar{\psi}^\beta(2)\psi^\beta(3)\psi^\alpha(4) \tag{30}$$

In the same manner we find

$$\mathcal{L}_{\rm cs2} = t^1_{\alpha\beta}(g^A\hat{I}+g^S\hat{T})\bar{\psi}^\alpha(1)\bar{\psi}^\beta(2)\psi^\alpha(3)\psi^\beta(4) \tag{31}$$

Using the symmetry properties of the spin operators and changing the dummy variables, it is easy to see that the term $\mathcal{L}_{\rm cs1}$ results in the same expression for the action [cf. Eq.(16)] as $\mathcal{L}_{\rm cs2}$, so $S_{\rm fb}=2S_{\rm cs2}$. Applying then the Fierz identity (10) [cf. also definitions (7)] for the operators $\hat{I},\hat{T}$ in case of $SU(2)$, and using the conservation law for momentum-frequency such that $3=1+Q$, $4=2-Q$, we get

$$S_{\rm fb} = -\frac{1}{4}t^1_{\alpha\beta}\int_Q\Big(g_c\rho^\alpha(Q)\rho^\beta(-Q)+4g_sS^\alpha_a(Q)S^\beta_a(-Q)\Big) \tag{32}$$

where we introduced the operators of the chiral (i.e., left/right) charge and of the chiral a-component of spin as

$$\rho^\alpha(Q) = \int_1\bar{\psi}^\alpha_\beta(1)\psi^\alpha_\beta(1+Q) \tag{33a}$$

$$S^\alpha_a(Q) = \frac{1}{2}\int_1\bar{\psi}^\alpha_\beta(1)\lambda^a_{\beta\gamma}\psi^\alpha_\gamma(1+Q) \tag{33b}$$

Note that in the above formulas there are no sums over α. We have also defined the charge and spin couplings:

$$g_c = g^S-3g^A \tag{34a}$$

$$g_s = -g^S-g^A \tag{34b}$$

It is worth noting that although there is no one-to-one correspondence between 1D couplings (13a,b) and the vertex components Γ^A,Γ^S [the latter in 1D are rather products of corresponding couplings and operators in the chiral space, as can be seen from comparison of Eqs.(8,25)], the definitions for the components which couple separated charge or spin modes (11) hold for the chiral ones (34). It is also useful to give the relationship between our constants and the standard (dimensionful) g-ology couplings: $g_c=2g_2-g_1$, $g_s=-g_1$.

The term $S_{\rm uc}$ of the total quatric interaction generated by the contact coupling at the same Fermi point (g_4) and the Umklapp coupling (g_3) can be written as

$$\begin{aligned}S_{\rm uc} = &-\frac{g_4}{4\cdot 2}\int_Q\Big(\rho^\alpha(Q)\rho^\alpha(-Q)-4S^\alpha_a(Q)S^\alpha_a(-Q)\Big) \\ &-\frac{g_3}{4\cdot 2}t^1_{\alpha\beta}\int_{1,2,Q}\Big(\delta_{\gamma\nu}\delta_{\sigma\varepsilon}-\lambda^a_{\gamma\nu}\lambda^a_{\sigma\varepsilon}\Big)\bar{\psi}^\alpha_\gamma(1)\psi^\beta_\nu(1+Q)\cdot\bar{\psi}^\alpha_\sigma(2)\psi^\beta_\varepsilon(2-Q)\end{aligned} \tag{35}$$

The way we write the Umklapp contribution is to reinstate the known fact that since g_3 couples fields with different chiralities, it cannot be represented in terms of the local chiral charge or spin operators.

D. Wilson-Kadanoff renormalization group for the chiral effective action

In this study we apply the original Wilson-Kadanoff momentum-space Renormalization Group scheme [1, 2] to the effective action with the quartic interaction containing four coupling constants. This interaction in the chiral formalism is given by Eqs. (25,26). In that formalism all the constraints coming from the original two-point geometry of the Fermi surface, and consequently, occurrence of the two types (left/right) of fermion fields and of Green's functions, are taken care of by the appropriate summations over chiral indices. In applying the RG procedure we successively integrate out the Grassmannian fields in the phase space of the small momenta k_i (12). The latter, like in the quantum or classical φ^4-theories, can be seen now as having common origin towards which we eliminate modes in the k-space.

We start with the effective action (25,26) having momenta restricted by the initial (bare) ultra-violet (UV) cutoff Λ_0 (15). After N steps of the mode elimination ($N \gg 1$), we end up with the cutoff Λ chosen such that:

$$\frac{\Lambda}{\Lambda_0} \ll 1, \quad \frac{v_F \Lambda}{T} \gg 1 \tag{36}$$

(We choose the RG scheme without rescaling of the cutoff.) Each step consists of mode integration within the infinitesimal shell Δ in the k-space, where

$$\Delta \equiv \frac{\Lambda_0 - \Lambda}{N} \tag{37}$$

(the equidistant step is chosen for simplicity only) such that after n steps the UV cutoff Λ_n is

$$\Lambda_n = \Lambda_0 - n\Delta, \quad 1 \leq n \leq N \quad (\Lambda_N \equiv \Lambda) \tag{38}$$

We define the n-th shell in the momentum space $\mathcal{S}_n$ as

$$\mathcal{S}_n \equiv [-\Lambda_{n-1}, -\Lambda_n] \cup [\Lambda_n, \Lambda_{n-1}] \equiv \mathcal{S}_n^- \cup \mathcal{S}_n^+ \tag{39}$$

In the final results given in the following sections we will smoothly take continuous limit $\Delta \to 0$ ($N \to \infty$) such that relationship (37) holds. Then the lowering cutoff Λ will be determined by the continuous RG flow parameter l defined as:

$$\Lambda(l) = \Lambda_0 \mathrm{e}^{-l} \tag{40}$$

As it was discussed in the closely related earlier study of the g-ology model [9], the straightforward application of the Wilson-Kadanoff RG beyond one-loop level encounters some difficulties. They stem from the constraint on the momenta to be integrated out at the n-th step to lie within the shell $\mathcal{S}_n$, and on the total momentum flowing through a given graph to conserve. It was shown in Ref. [9] that the solution of this problem consistent with the logic of the WK RG can be found when multi-loop graphs (the standard ones for the field-theoretical

RG) renormalizing action's vertices are obtained through cascades of contractions at different steps of the RG procedure. In this study we refine the "cascade scheme" of the RG calculations put forward in Ref. [9] for the g-ology model. We show that the aforementioned constraints on the momenta can be cast in terms of the "selection rules" for the numbers of steps entering a given cascade of contractions. Summations over all allowed types of cascades provides the results particularly illuminating for understanding the origin of the (logarithmic) equivalence of the WK and field-theoretic RG versions.

III. SELF-ENERGY AT THE TWO-LOOP LEVEL

A. Cascades of contractions and kinematic constraints

We use the standard definition for the field renormalization constant relating it to the self-energy (assuming that the analytical continuation from Matsubara frequencies is done):

$$Z^{-1} = 1 - \frac{\partial \Sigma_\alpha(k,\omega)}{\partial \omega}\Big|_{k\to 0}^{\omega\to 0} \tag{41}$$

It is easy to show that in our model Z does not dependent on the chirality index. The first correction to Z comes from the two-loop "sunrise" self-energy diagram. However, in the WK RG scheme such a diagram if obtained in the second order by a contraction of three legs of the four-leg interaction (16) with itself, gives a vanishingly small contribution. This is due to the momentum constraints discussed above. (See also Ref. [9] for more details.) The graphs we are looking for can come only from two types of cascades of contractions generated by the mode elimination of the original action (16): 3-step and 2-step cascades depicted in Fig. 1. *3-step cascade* (Fig. 1a) is generated (in the second order over interaction) as follows: (i) at the n-th step of the mode elimination the four-point vertex is contracted with itself to generate the six-leg vertex; (ii) m steps after [i.e. at the $(n+m)$-th step] two legs of this vertex are contracted; (iii) at the $(n+m+k)$-th step two other legs are contracted resulting in the final correction to the two-leg vertex (i.e., one-particle Green's function). *2-step cascade* (Fig. 1b) is generated as follows: (i) at the n-th step two pairs of legs of the four-point vertices are contracted; (ii) at the $(n+m)$-th step two more legs are contracted. The above description of the cascades was very schematic and illustrative. We did not take care of the kinematics of diagrams (that is why we did not indicate the momentum directions in the graphs of Fig. 1), and the integers numerating the steps are unrelated and free to take any values restricted only by the total number of steps of the RG procedure, i.e., $1 \le n \le n+m \le n+m+k \le N$.[2]

To proceed with the further analysis of the pertinent cascades let us consider the renormalization of the one-particle Green's function at $k = \Lambda$. As the RG flows towards the fixed point ($\Lambda \to 0$) this quantity will provide us with the field renormalization constant Z (41). For this purpose we consider the terms generated by the two types of cascades described above renormalizing the coefficient of the action's Grassmannian binomial $\bar{\psi}(1)\psi(1)$. Diagrammatically they are shown in Fig. 2. Analysis reveals that there are three kinematically non-equivalent graphs (a, b, c in that figure) generated by the 3-step cascades and two graphs

[2] Note that 2-step cascade or "1-step cascade" (i.e., simple contraction) can be considered as special cases of a 3-step cascade if we allow the integers m, k to take zero values.

(d, e) from 2-step cascades. We choose the external momentum

$$k_1 = \Lambda_N \equiv \Lambda \tag{42}$$

and the other external variables (chirality, spin, frequency) are not specified at this point. For the further applications we approximate

$$\Lambda = L\Delta \tag{43}$$

where L is an integer ($1 \ll L \ll N$). The error $\mathcal{O}(\Delta)$ of the representation (43) disappears when we eventually take the limit $\Delta \to 0$.

Let us start with the kinematics of the first three graphs. We find that for each of these graphs there are two solutions compatible with the constraints imposed by the WK procedure and the momentum conservation law. They are given in Table I.

Table I: *Solutions for the momenta of the three graphs in Fig. 2 compatible with the kinematic constraints.*

Graph	a	a	b	b	c	c
Solution	I	II	I	II	I	II
m'=	m	m-2L	m	m-2L	m	m-2L
$k_2 \in$	$\mathcal{S}^-_{N-m}$	$\mathcal{S}^+_{N-m+2L}$	$\mathcal{S}^+_n$	$\mathcal{S}^-_n$	$\mathcal{S}^-_{n+m}$	$\mathcal{S}^+_{n+m}$
$k_3 \in$	$\mathcal{S}^-_n$	$\mathcal{S}^+_n$	$\mathcal{S}^+_{N-m}$	$\mathcal{S}^-_{N-m+2L}$	$\mathcal{S}^+_{N-m}$	$\mathcal{S}^-_{N-m+2L}$
$k_4 \in$	$\mathcal{S}^+_{n+m}$	$\mathcal{S}^-_{n+m}$	$\mathcal{S}^+_{n+m}$	$\mathcal{S}^-_{n+m}$	$\mathcal{S}^-_n$	$\mathcal{S}^+_n$

The ranges for the integers n, m satisfying the solutions I, II are:

$$I\ (a,b,c): \quad 1 \le n \le N - 2m; \qquad 1 \le m \le \frac{N}{2} \tag{44a}$$

$$II\ (a,b,c): \quad 1 \le n \le N + 2(L-m);\ 2L < m \le \frac{N}{2} + L \tag{44b}$$

Thus in order to obtain the total contribution of these cascade-generated graphs to the self-energy we have to integrate two independent momenta in each graph over available range (i.e. two possible configurations I, II for each graph) and to sum over all allowed types of cascades parameterized by (n, m) within the ranges (44). (And of course, there are always straightforward summations over other variables, i.e., chirality, spin, frequency which take all available values.)

We have not shown in Table 1 available kinematic solutions for the 2-step cascade graphs d, e, since their contribution is negligible in comparison to that of a-c. Indeed, as can be shown from the results below, the graphs d, e as well as a-c *at a fixed m* give the contributions $\mathcal{O}(\Delta/\Lambda)$ to the constant Z. However the extra sum over m renders the latter logarithmic $\mathcal{O}(\ln \frac{\Lambda_0}{\Lambda})$, while the former do not have this extra sum and thus strictly disappear in the limit $\Delta \to 0$. For the same reason we drop some extra solutions for the graphs a-c which occur only under special relationships between n and m (i.e., there is no double sum over n, m): they give vanishing contributions.[3]

[3] In the light of the previous comment (see the footnote on p. 10) it is clear that special configurations (or

B. Two-loop calculations

Now we can proceed with the RG calculations via a straightforward evaluation of the graphs from Fig. 2. For certainty we fix the external chiral index of those graphs to be 2, i.e. corresponding to the right component of the Grassmannian field. Since graph's contributions in the spin space are diagonal and spin-independent, the external spin can be "up" or "down". After summation over chiral and spin indices we obtain for the sunrise graph contribution $\mathrm{F}_+(1)$ (here plus stands to indicate our choice of the external chiral index):

$$\mathrm{F}_+(1) = \int_{(2,3,4)} \Big[\frac{1}{2}\big(g_c^2 + 3g_s^2\big)\cdot \mathcal{F}_+^{cs} + 2g_3^2 \cdot \mathcal{F}_+^{u} + 2g_4^2 \cdot \mathcal{F}_+^{4}\Big]\, \delta^{(1+1)}(1+2-3-4) \tag{45}$$

where thin variables signify momenta and frequencies, i.e., the only ones left, and

$$\mathcal{F}_+^{cs} \equiv G_-(2)\big[G_-(3)G_+(4) + G_+(3)G_-(4)\big] \tag{46a}$$
$$\mathcal{F}_+^{u} \equiv G_+(2)G_-(3)G_-(4) \tag{46b}$$
$$\mathcal{F}_+^{4} \equiv G_+(2)G_+(3)G_+(4) \tag{46c}$$

Note that until the integration ranges for the momenta k_2, k_3, k_4 are specified, the same analytical expression $\mathrm{F}_+(1)$ (45) corresponds to the *each of graphs* depicted in Fig. 2.

The following summation of Matsubara frequencies in (45) is straightforward. Due to conditions (36) we approximate the occurring hyperbolic functions up to exponentially small terms $\mathcal{O}(\exp(-\Lambda/T))$. With this accuracy we drop all contributions from the term $\mathcal{F}_+^4$. Analysis of the available kinematic configurations from Table 1 for other terms shows that some of them are also exponentially small, so we put

$$\mathcal{F}_+^{cs}\big|_{bI,II} = 0 \tag{47a}$$
$$\mathcal{F}_+^{u}\big|_{aI,II} = 0 \tag{47b}$$
$$\mathcal{F}_+^{u}\big|_{cI,II} = 0 \tag{47c}$$

Our calculations show that the term $\mathcal{F}_+^{cs}$ evaluated for the configurations of the graph a (solutions I, II) and c (I, II) gives four equal contributions to the self-energy. Analogously, two contributions of $\mathcal{F}_+^{u}$ from b (I, II) are equal to each other. In order to demonstrate how these calculations are done, let us consider as an example $\mathcal{F}_+^{cs}$ for the configuration (a, I). To obtain its total contribution to the self-energy, we have to to integrate two independent momenta within the ranges indicated in Table I for fixed n, m and then to sum over all available cascades (a, I) according to (44a). This gives: [4]

$$\Sigma_+^{cs}(1)\Big|_{a1} = \frac{v_F}{16}\big(g_c^2 + 3g_s^2\big)\sum_{m=1}^{N/2}\sum_{n=1}^{N-2m}\int_{-\Lambda-m\Delta}^{-\Lambda-m\Delta+\Delta} dk_2 \int_{\Lambda_n-m\Delta}^{\Lambda_n-m\Delta+\Delta} \frac{dk_4}{a_+ - k_2 + k_4} \tag{48}$$

"lower-order" cascades) are in fact recovered in the double integrals appearing in the limit $\Delta \to 0$ as some points or lines, i.e., manifolds of inferior measure.

[4] Strictly speaking, couplings in the sunrise graphs depend on the smallest shell number, i.e., n. By pulling them out of sums and integrals, as should be clear from the content of this section, we actually approximate them by their values at the largest shell number (i.e., at Λ). This approximation (called "local" in Ref.[9]) is common for all RG schemes, and in any case possible corrections to it lie beyond the two-loop level.

where

$$\frac{1}{a_+} \equiv 2v_F G_{0,+}(1) \tag{49}$$

In Eq. (48) and in the following we use dimensionless couplings absorbing the density of states factor in their definition, i.e.,

$$\frac{g_\sharp}{\pi v_F} \mapsto g_\sharp \tag{50}$$

In the limit $\Delta \to 0$ the sums above neatly combine into a simple double integral

$$\Sigma_+^{cs}(1)\Big|_{a1} = \frac{v_F}{16}\big(g_c^2 + 3g_s^2\big) \int_{-\frac{1}{2}(\Lambda_0+\Lambda)}^{-\Lambda} dk_2 \int_{-k_2}^{\Lambda_0+\Lambda+k_2} \frac{dk_4}{a_+ - k_2 + k_4} \tag{51}$$

which gives

$$\frac{\partial \Sigma_+^{cs}(0)}{\partial \omega}\bigg|_{a1} = -\frac{g_c^2 + 3g_s^2}{4\cdot 16}\big(\ln\frac{\Lambda_0}{\Lambda} + ...\big) \tag{52}$$

where the omitted terms $const + \mathcal{O}(\Lambda/\Lambda_0)$ are irrelevant for the RG flow equations. Combining evaluated in the same way other contributions and using the definitions (40,41), we obtain the two-loop RG equation

$$\frac{\partial \ln Z}{\partial l} = -\frac{1}{16}(g_c^2 + 3g_s^2 + 2g_3^2) \tag{53}$$

This equation was first obtained in Ref.[6].

C. Wilson-Kadanoff vs field-theoretic schemes

In order to get more insights from the obtained results, let us first rewrite some of the previous formulas. Using the transfer momentum vector $q = k_2 - k_4$ in Eq.(51), we get

$$\Sigma_+^{cs}(1)\Big|_{a1} = \frac{v_F}{16}\big(g_c^2 + 3g_s^2\big) \int_{-\frac{1}{2}\Lambda_0}^{-\Lambda} dk \int_{-\Lambda_0}^{2k} \frac{dq}{a_+ - q} \tag{54}$$

In the above equation we dropped the index of the vector k_2 and neglected terms $\Lambda \ll \Lambda_0$ in the limits of integrals, since we are eventually interested only in the $\Lambda \to 0$ limit. Other three non-zero contributions [cf. Eq.(47a)] to the *cs*-term of the self-energy after analogous variable changes can be reduced to the form (54) but with different integration ranges. Combined together, these contributions can be written as:

$$\Sigma_+^{cs}(1) = \frac{v_F}{16}\big(g_c^2 + 3g_s^2\big) \int_{-\frac{1}{2}\Lambda_0}^{\frac{1}{2}\Lambda_0} dk\Theta(k^2 \geq \Lambda^2) \int_{-\Lambda_0}^{\Lambda_0} \frac{dq\Theta(q^2 \geq 4k^2)}{a_+ - q} \tag{55}$$

where Θ is the event (Heaviside) function.

Thus, by applying the canonical Wilson-Kadanoff scheme where all momenta in the diagrams lie strictly within an infinitesimal shell at each step of the RG procedure, and by summing all pertinent infinitesimal contributions through singling out kinematically-allowed cascades, we end up with results which could have been obtained in the field-theoretic

scheme. As one can see, formula (55) for the self-energy resembles the one derived in the RG scheme where momenta are let to run freely within a whole band restricted only by the IR and UV cutoffs.

To sharpen the last statement, let us derive now the self-energy in the field-theoretic RG scheme with the cutoff regularization. (Thorough description of various field-theoretic RG approaches can be found, e.g., in Ref.[14].) Let us assume that we have the same bare effective action as we used before. Since the theory is logarithmical, we regularize divergent integrals by introducing IR and UV cutoffs. We assume that they satisfy the same conditions as those for the WK effective action (36). Since *a priori* the cutoffs in the field-theoretic and WK approaches are not the same, we will mark the former with tildes.[5] Contrary to the WK scheme, in the field-theoretic approach the self-energy contribution we are looking for: *(i)* comes from the *only one* sunrise graph as those depicted in Fig. 2; *(ii)* independent momenta in the graph are restricted by the model cutoffs only ; *(iii)* the graph has a combinatorial factor 1/2. All the summations before the final momentum integrations in this graph lead to the same formulas as in the previous subsection (except the overall factor 1/2). We choose a couple of independent momenta k_i restricted by the cutoffs $\tilde{\Lambda}, \tilde{\Lambda}_0$. It can be shown that the term of the self-energy involving charge and spin couplings can be brought to the form (55) with $\tilde{\Lambda} \mapsto \Lambda$, $\tilde{\Lambda}_0 \mapsto \Lambda_0$ up to $\mathcal{O}(\tilde{\Lambda}/\tilde{\Lambda}_0)$. With the same accuracy the self-energy Umklapp terms coincide in the WK and field-theoretic approaches. Thus both schemes result in the same leading $\ln(\Lambda_0/\Lambda)$ term in the derivative of the self-energy with respect to the frequency, and therefore to the same RG equation (53).

The relationship between the two RG schemes can be seen even in a simpler way in the limit $\Lambda \to 0$, i.e., the fixed point limit we are always interested in. Let us draw the regions of momenta integrations corresponding to the solutions from Table I summed over available n and m. As a couple of independent momenta we choose (k_3, k_4). These regions are shown in Fig. 3. Let us remind also that while showing kinematically non-equivalent cascades (a-c) in Fig. 2 we have used the (anti)symmetry of the vertex, and, correspondingly, that of graph's contributions under the exchange $(3 \leftrightarrow 4)$. So the sum of these three graphs can also be written as $(a+b+c) = \frac{1}{2}(a+b+c+a'+b'+c')$, where the primed graphs correspond to the above exchange. As one can see from Fig. 3 the regions for unprimed and primed solutions (the primed solutions are obtained from their unprimed counterparts by the reflection over the main diagonal), fill completely the hexagon shown in bold. The latter is nothing but the whole phase space of the sunrise graph

$$\mathcal{S}_{\rm restr}: \ |k_i| \le \Lambda_0, \ i = 2,3,4; \ k_1 = 0. \tag{56}$$

Now assuming that the summations and integrations commute we can write the total sunrise self-energy correction $\Sigma^{\rm casc}_{\rm sr}$ resulting from the sum of three kinematically distinct graphs 2a-c over two solutions for each graph and over all available cascades as a single term

$$\Sigma^{\rm casc}_{\rm sr}(1) = \frac{1}{2}\int_{(2,3,4);k_i\in\mathcal{S}_{\rm restr}} \Gamma(12,34)G(2)G(3)G(4)\Gamma(34,12)\ \delta^{(1+1)}(1+2-3-4) \tag{57}$$

Here we came back to the original thin variables comprising chiral and spin indices, Matsubara frequencies, and momenta $(\omega_1, k_1 \to 0)$. Thus the self-energy correction has the same

[5] For the IR cutoff $\tilde{\Lambda}$ to be the smallest scale of the problem we will work with the theory in the zero-temperature limit. For the following comparisons note that the second condition (36) effectively brings the WK RG results to the zero-temperature limit as well.

analytical form as the one written in the cutoff field-theoretic approach. In the latter however, after removing one momentum by the delta-function (e.g., k_2) only two independent momenta are explicitly restricted by Λ_0. This results in the contributions from the extra states forbidden by the whole phase space constraints. These extra states lie in the triangles in the first and third quadrants of the (k_3, k_4)-plane (cf. Fig. 3). In the logarithmic theory as the one we are dealing with, integration over these forbidden states may result in only the finite terms to the self-energy correction, thus leaving the RG equation (53) unaffected.[6]

The phase space mapping of Fig. 3 holds in the fixed-point limit $\Lambda \to 0$ at non-zero temperature as well. Thus the temperature effects can be calculated from the UV cutoff RG scheme upon integration of the all phase space restricted by the hexagon in Fig. 3.[7] As it should be clear, this is not equivalent either to calculation within WK RG stopped at some l^* when $v_F\Lambda(l^*) \sim T$, or within the two-cutoffs RG with the IR cutoff provided by T: such two ways of calculations give, strictly speaking, approximations only.

IV. COUPLINGS AT THE TWO-LOOP LEVEL

After explaining most of technicalities in the previous section, we will be brief in presenting the results for the RG coupling equations. Let us first write the two-loop perturbative expansion for the four-point 1PI vertex. It is depicted graphically in Fig. 4. (The tadpole self-energy corrections are absorbed in the one-particle Green's functions renormalizations.) We calculate the couplings from $\Gamma(12, 34)$ at

$$k_i = 0,\ \omega_i = \omega_\circ\ (i = 1, ..4) \tag{58}$$

where $\omega_\circ$ is the minimal Matsubara fermionic frequency. The latter is set to zero after appropriate analytical continuation. The couplings are extracted from Γ by convolutions [cf. Eqs.(27) and below]. The limits (58) considerably reduce the number of cascades to take into account while calculating the renormalized couplings.

One-loop corrections are generated by a simple contraction shown in the first line of Fig. 1b. After summations over the shell number these contributions reduce to three one-loop graphs with the signs and factors as in the pertubrative expansion in Fig. 4 and the loop momentum $\Lambda \leq |k| \leq \Lambda_0$.

Pertinent double-loop graphs are generated by the 2-step cascade as follows: at the n-th step a simple one loop is generated (cf. first line of Fig. 1b) and at the m-th step the left (or right) pair of legs of this graph is contracted with the four-leg vertex. The shell numbers n and m are independent and can take any value from 1 to N. The sums of these cascades result in the three double-loop graphs (DL) as they stand in the second line in Fig. 4 with the loop momenta restricted by $\Lambda \leq |k| \leq \Lambda_0$.

---

[6] It is possible, (e.g., it happens for the component Σ^{cs}) that summation over frequencies bringing the Fermi functions into play, suppresses completely the differences between two schemes coming from the extra states. For Σ^{cs} the contributions from the first and third quadrants are completely eliminated by the Fermi functions [cf. Eq.(47a)]. But generically there are no reasons for that, and the Umklapp contribution provides a counterexample for Σ^{cs}. Cf. Eqs.(47b,c).

[7] Note, however that the explicit form of the flow equations, i.e., the Gell-Mann–Low functions, derived here in the limit $T \to 0$, are modified at $T \neq 0$ when decreasing cutoff $\Lambda(l)$ reaches the scale provided by the temperature.

The two-loop graphs combined in the groups (ZZ, ZC, CZ) in Fig. 4 are generated by the 3-step cascades. For concreteness let us take the first graph from the group ZZ. For each type of this loop configuration with a fixed position of external variables (top left in Fig. 5) there are six graphs corresponding to all possible types of the 3-step contractions shown in this figure. Direct inspection shows that the sign and combinatorial factor of all these six graphs are the same and coincide with those of their counterpart in the perturbative expansion in Fig. 4. Due to conditions (58) we retain only such cascades that the legs of the vertex α are contracted at the same step. From the conservation law the momenta k_5, k_6 are equal (opposite for the CZ graphs), so the phase space constraints near the vertex α are satisfied trivially. To find the allowed kinematic solutions from the second independent momentum conservation (e.g., at the vertex β of this graph) we can use directly the results of the previous section. Indeed, if we identify k_2, k_8, k_5, k_7 of the graphs in Fig. 5 with k_1, k_2, k_3, k_4 of Fig. 2, respectively, we recover the situation analysed previously for the self-energy graphs. The kinematic solutions for the graphs of Fig. 5 can be taken from Table I (in the limit $L = 0$) as follows: $i \mapsto a$, $ii \mapsto c'$, $iii \mapsto a'$, $iv \mapsto b'$, $v \mapsto c$, $vi \mapsto b$. Then contributions $i - vi$ (cf. footnote on p. 12) can be combined into a single graph (top left in Fig. 5) with two independent momenta lying in the phase space shown in Fig. 3. Analogous conclusions can be reached for other graphs of the groups ZZ, ZC, CZ. Thus, provided the stipulated above phase space of each graph, the renormalization of the vertex after mode elimination between Λ and Λ_0 ($\Lambda \to 0$) is given by Fig. 4.

The rest of the calculations is straightforward. We introduce the renormalized (dimensionless) couplings as follows:

$$g_\sharp = Z^2 Z_\sharp^{-1} g_\sharp^{(\mathrm{bare})} \tag{59}$$

The vertex renormalization constants $Z_\sharp^{-1}$ in terms of $g_\sharp$ are found to be:

$$Z_c^{-1} \;=\; 1 + \frac{g_3^2}{g_c} l + \frac{1}{8}(g_c^2 + 3g_s^2 - 2g_3^2) l - g_3^2\big(1 - \frac{g_3^2}{g_c^2}\big) l^2 \tag{60a}$$

$$Z_s^{-1} \;=\; 1 + g_s l + \frac{1}{8}(g_c^2 - g_s^2 + 2g_3^2) l \tag{60b}$$

$$Z_3^{-1} \;=\; 1 + g_c l - \frac{1}{8}(g_c^2 - 3g_s^2) l + \frac{1}{2}(g_c^2 - g_3^2) l^2 \tag{60c}$$

Combining the equations

$$\frac{d \ln g_\sharp}{dl} = 2\frac{\partial \ln Z}{\partial l} + \frac{\partial \ln Z_\sharp^{-1}}{\partial l} + \sum_{i=c,s,3} g_i \frac{\partial \ln Z_\sharp^{-1}}{\partial g_i} \frac{d \ln g_i}{dl} \tag{61}$$

with Eqs.(53,60) we obtain the RG flow equations for couplings:

$$\frac{dg_c}{dl} \;=\; g_3^2 - \frac{1}{2} g_c g_3^2 \tag{62a}$$

$$\frac{dg_s}{dl} \;=\; g_s^2 - \frac{1}{2} g_s^3 \tag{62b}$$

$$\frac{dg_3}{dl} \;=\; g_3 g_c - \frac{1}{4} g_3 (g_3^2 + g_c^2) \tag{62c}$$

These equations were obtained earlier within the field-theoretic RG analysis [6]. Note that in the above equations we dropped all the contributions from g_4 assuming that they can be absorbed in the renormalization of Fermi velocities. (See, e.g., Ref. [7] and more references therein.)

V. CONCLUSIONS

The equivalence of the RG flow equations in the WK and field-theoretic schemes at the two-loop level is proven explicitly for the 1D g-ology model. To obtain the higher-order RG equations within the canonical WK approach, it is crucial to sum over all available cascades of contaractions occurring at the infinitesimal steps of the WK procedure. Moreover, in the fixed-point limit $\Lambda \to 0$ the diagrammatics of the WK RG summed over all cascades is shown to be the same as that of the field-theoretic RG with the cutoff regularization and restricted phase space.

Generalizations for the cases of classical or quantum bosonic and fermionic fields and higher dimensions are straightforward within the developed technique, resulting in the same conclusion about the diagrammatics, provided that the relevant phase space of those fields (i.e., the low-energy sector) can be brought to the same origin.

If the latter condition can not be satisfied easily, like, e.g, for the low-energy sector of higher dimensional condensed-matter fermions possessing a Fermi surface, the proof of equivalence is not a straightforward extension within the proposed approach, and more explicit work is needed to demonstrate it. However we conjecture that even in that case the summation over cascades within the WK RG tantamount to applying the field-theoretic RG with a (bare) UV cutoff for the low-energy sector and locally-imposed phase-space constraints of the integrated momenta. (For the examples of how these constraints may be realized, see the review by Shankar [5].)

At the level of three loops and higher, different RG schemes may result in different flow equations. Within the present approach, it follows from the necessity to take into account the dependence of running couplings on the shell number in higher orders (cf. footnote on p. 12). So various cascade contributions could not be "compactified" in a single "field-theoretic" graph as it occurs at the two-loop level. The latter conclusion is hardly surprising, since the differences in the Gell-Mann–Low functions in higher orders are known to occur even within different versions of the field-theoretic RG. (See, e.g, Ref.[14]. In the context of the 1D g-ology, see also Ref.[15] for the discussion of the bandwidth- and transfer-cutoff regularizations in higher orders of RG.)

In condensed-matter problems, where the bare UV cutoff Λ_0 might be a meaningful scale and other scales (e.g., T, K_F) may be present as well, the WK RG scheme should be applied, as the one which is just an exact way to to integrate the partition function [1, 2]. The WK RG does not rely on any assumptions of the scales involved, scaling/logarithmicity of theory, etc, and includes contributions only from the states lying within the phase space of the problem. This allows to control the results (at least in principle) in all orders. In practical terms, after summations over all cascades the WK scheme asymptotically maps to the much easier to handle field-theoretic RG (up to three loops) with forbidden states excluded. We did not verify whether possible simplifications of the WK scheme can be done in even higher orders, but going beyond two-loop level is a formidable problem in any case.

Acknowledgments

G.Y.C. is grateful to M.E. Fisher and A.M. Tsvelik for helpful discussions, and to McGill University for hospitality. C.B. thanks R. Wortis for important remarks at the early stage of this work. This work is supported by NSERC (Canada), FCAR (Qébec), and German

Science Foundation.

---

[1] K.G. Wilson and J. Kogut, Phys. Rep. **12C**, 75 (1974).

[2] K.G. Wilson, Rev. Mod. Phys. **47**, 773 (1975); *ibid* **55**, 583 (1983).

[3] L.P. Kadanoff, Physics **2**, 263 (1966).

[4] E. Brézin, J.C. Le Guillou, and J. Zinn-Justin, in *Phase Transitions and Critical Phenomena*, v. 6, eds. C. Domb and M.S. Green (Academic Press, New York, 1976).

[5] R. Shankar, Rev. Mod. Phys. **66**, 129 (1994).

[6] M. Kimura, Prog. Theor. Phys. **53**, 955 (1975).

[7] J. Sólyom, Adv. Phys. **28**, 201 (1979).

[8] C. Bourbonnais and L. G. Caron, Int. J. Mod. Phys. B **5**, 1033 (1991); C. Bourbonnais, in *Les Houches, Session LVI (1991), Strongly interacting fermions and high-T_c superconductivity*, edited by B. Doucot and J. Zinn-Justin (Elsevier Science, Amsterdam, 1995), p. 307.

[9] C. Bourbonnais, B. Guay, and R. Wortis, in *Theoretical methods for strongly correlated electrons*, edited by A. M. Tremblay, D. Sénéchal, A. Ruckenstein, and C. Bourbonnais (Springer, Heidelberg, 2003); cond-mat/0204163.

[10] J.W. Negele and H. Orland, *Quantum Many-Particle Systems* (Addison-Wesley, New York, 1988).

[11] G.Y. Chitov and D. Sénéchal, Phys. Rev. B **52**, 13487 (1995).

[12] J. Voit, Rep. Prog. Phys. **58**, 977 (1995).

[13] I. E. Dzyaloshinskii and A. I. Larkin, Sov. Phys. JETP, **34**, 422, (1972).

[14] J. Zinn-Justin, *Quantum Field Theory and Critical Phenomena*, Third Edition, (Clarendon Press, Oxford, 1999).

[15] E. H. Rezayi, J. Sak, and S. Talukdar, Phys. Rev. B **19**, 4757 (1979).

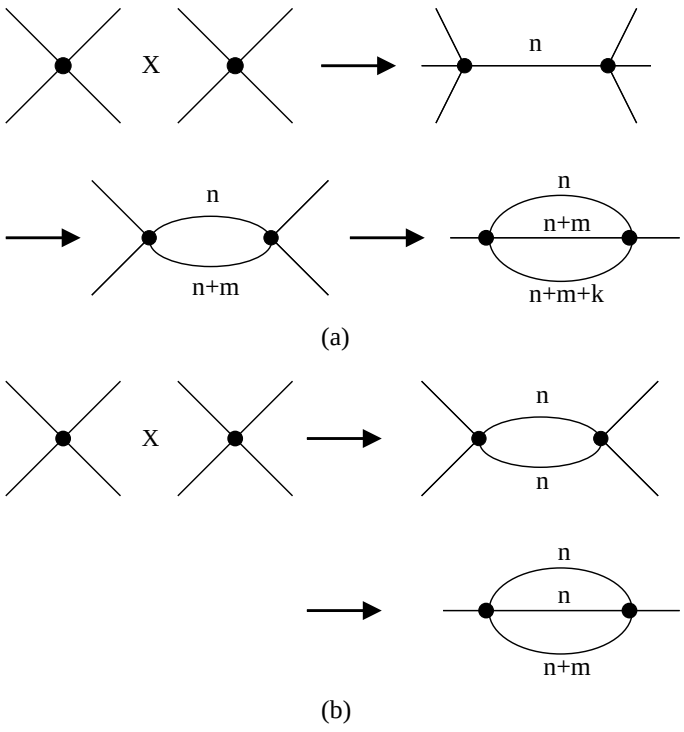

FIG. 1: Diagrammatic representation of the two types of cascades of contractions in the second order over interaction. (a): 3-step cascade; contractions are done at the steps $n, n+m, n+m+k$. (b): 2-step cascade; contractions are done at the steps n and $n+m$.

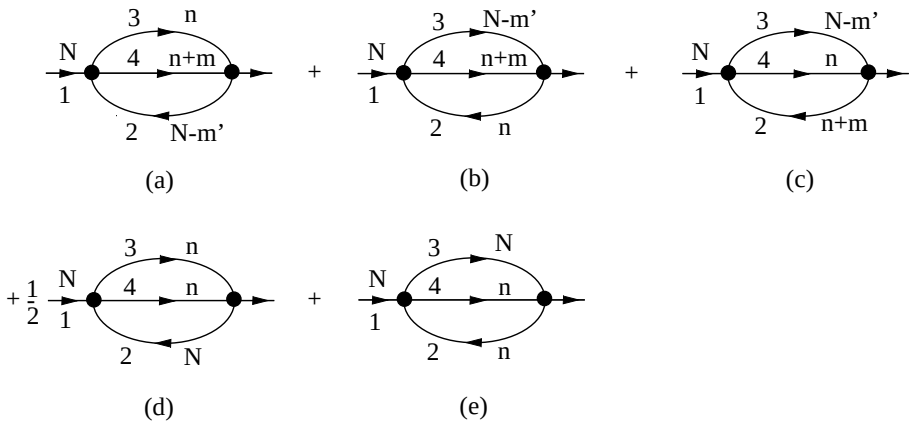

FIG. 2: Two-loop kinematically-distinct self-energy diagrams generated after N steps of the Wilson-Kadanoff procedure. Graphs $(a-c)$ are generated by the 3-step cascade (see Fig. 1a), $n < n+m < N-m'$; (d-e) by the 2-step cascade (see Fig. 1b). Integres shown near the composite variables $(1-4)$ indicate the shell number where the corresponding momenta are restricted to lie. The signs and combinatorial factors of the graphs stand as they enter the action's binomial term $\bar{\psi}(1)\psi(1)$. Implicit sum over all allowed $n, m(m')$ is assumed.

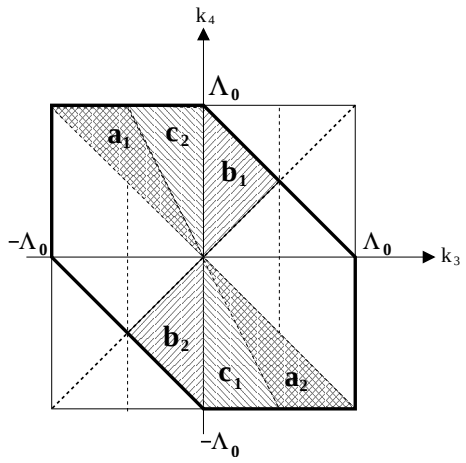

FIG. 3: Regions of momenta integrations corresponding to the solutions from Table I in the limit $\Lambda \to 0$. The regions for the primed solutions (not given explicitly in Table I) are obtained by reflection over the main diagonal (bold dashed line), so the whole set of 12 solutions fill completely the restricted phase space (56), i.e., the hexagon shown by the solid bold line. The vertical thin dashed lines are guides for an eye.

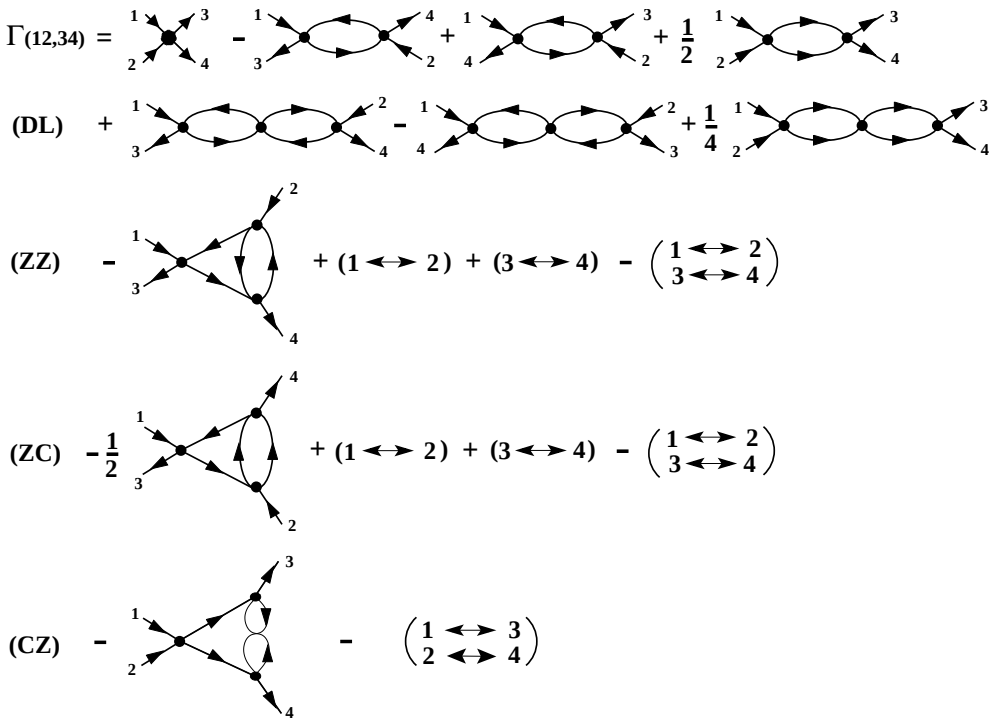

FIG. 4: Two-loop perturbative expansion for the four-point vertex. The tadpole self-energy corrections are absorbed by the Green's function renormalization. The vertex variables indicated by numbers comprise the complete set: chiral and spin indices, Matsubara frequencies, and momenta. For convenience the two-loop graphs are separated in four groups (DL, ZZ, ZC, CZ) discussed in the text. Note that in the graph CZ we depicted a twisted particle-hole loop, not a double loop.

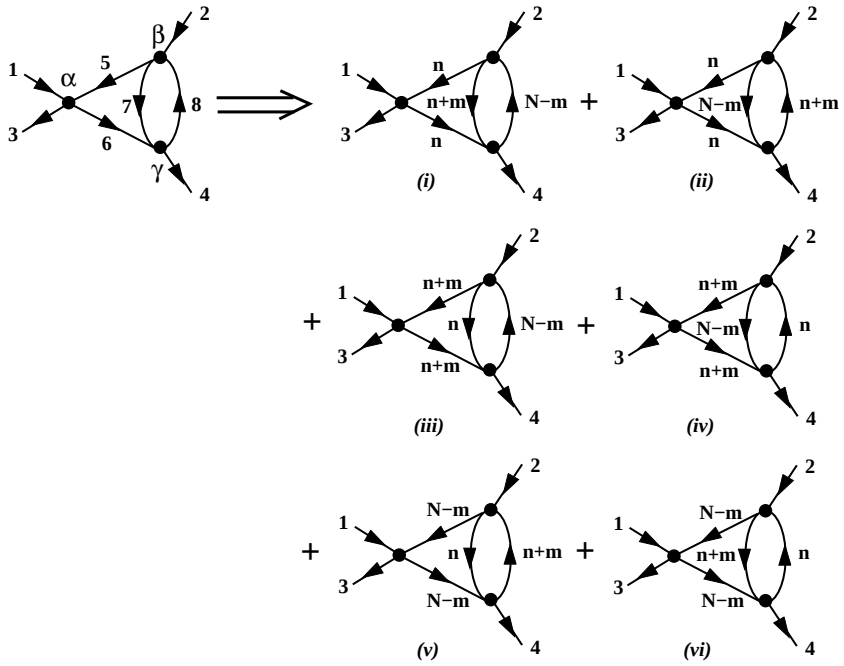

FIG. 5: 3-step cascades of contactions generating two-loop corrections (topology of the ZZ, ZC, CZ graphs) to $\Gamma(12,34)$ in the limit (58). As an example, six distinct cascades corresponding to the kinematics and the external legs configuration of the first graph from the group ZZ of Fig. 4, are shown. For the sake of space, the vertex labels and notations for the integrations dummy variables discussed in the text (the same for all depicted graphs), are explicitly indicated in the top left one only. The integers in the graphs *(i-vi)* show the shell numbers where momenta $(k_5,..,k_8)$ lie. Note that as in the case of the self-energy corrections (cf. Figs. 1-2), the 3-step cascades come from higher many-body interactions, themselves generated along the RG flow. In the graph *(i)*, taken as an example, the first contraction (step n) leads to a four-particle interaction, the second step n+m to a three-particle one, and the final third step N-m yields the two-particle interaction correction *(i)*.